Aust. J. Phys., 1988, **41**, 383–91

Use of Extinction Corrections in Neutron Diffraction Experiments*

A. Delapalme

Laboratoire Léon Brillouin (CEA-CNRS), CEN-Saclay,
91191 Gif-sur-Yvette, Cedex, France.

Abstract

The study of extinction by neutrons reveals many features of the extinction problem: theory and practical cases, polarised and unpolarised neutron cases. Special attention is given to the usual extinction corrections for neutron diffraction experiments, showing the relative importance of structure factor, wavelength, Lorentz factor, mosaic and the path of neutrons through the crystal. Two problems are reviewed: (a) how to detect the presence of extinction in both cases of a single crystal experiment with polarised and unpolarised neutrons; and (b) after experimental evidence for extinction in a neutron diffraction experiment, how to follow a reliable way to correct the neutron diffraction data in both cases of polarised and unpolarised neutron experiments. Some examples are given.

1. Introduction

Extinction can be treated through various models originating in either kinematical (intensity coupling) or dynamical (wave coupling) theories. The dynamical theory is the more general but can only be applied to crystals that are perfect or show only small distortions. The kinematical theory is the limit of the dynamical in the case of small coherent domains or short wavelengths; it is widely used in structural crystallography. For most crystals the situation is intermediate between these two extreme cases and extinction models are necessary to obtain precise Fourier components (structure factors) and the electronic and magnetic distribution in molecules and crystals.

Kato (1976) partially reconciled the two approaches, solving Takagi's (1969) equations in a statistical way and under definite conditions. For an optical coherence length τ smaller than the extinction distance Λ, he obtained intensity coupling equations which were shown to be identical with those employed to describe mosaic theories (Becker 1977). The solution to these equations has been examined by Zachariasen (1967), Werner (1974) and Becker and Coppens (1974; henceforth BC). For a more experimental viewpoint, the importance of collimation (Dietrich and Als-Nielsen 1965; Bogdanov and Menshikov 1976), the determination of mosaic (Schneider 1974), and the correlation between scale factor, thermal parameter and extinction must be examined in detail (Bonnet *et al.* 1976; henceforth BDBF) for the purpose of obtaining structure factors better than 1%.

* Paper presented at the International Symposium on Accuracy in Structure Factor Measurement, held at Warburton, Australia, 23–26 August 1987.

0004-9506/88/030383$03.00

Recently Kulda (1984, 1987) pointed out that the treatment based on the energy transport equation (ETE) (Zachariasen 1967, 1968) suffers from certain deficiencies, of which the most important seems to be its failure to describe primary extinction. But again, in the limit of secondary extinction and after consideration of the different approaches, it can be concluded that the use of ETE is physically correct, the remaining problem being to find an adequate expression for the coherent scattering cross section $\sigma(\epsilon)$.

The general situation of extinction models manifests itself as a difficult correspondence between theory and experiment, with the result that theoreticians are led, for the sake of simplicity, to use a phenomenological formalism in order to obtain formulae that can be built into a refinement program. New models have new parameters which give rise to new effects in the extinction corrections, but the phenomenological aspect of the solutions shows the difficulty of adequately describing what happens in real crystals.

Careful examination for the presence of extinction and for the validity of the corrections is then needed; often, one must test the adequacy of these extinction corrections.

2. Parameters of BC Formalism within the Limit of the Darwin Transfer Equations

We describe the features of the BC formalism to reveal the connection between the different parameters:

(1) The most important limitation is due to its kinematical nature; the model uses the ETE (see equations in BC 10a, b, c). The diffracting cross section per unit volume and intensity $\sigma(\epsilon)$ (where ϵ is any angular departure from the Bragg conditions) is assumed to be constant inside the crystal and dependent only on the size and shape of the average mosaic domain (BC 4). The domains are assumed to be of the same size and nearly spherical in shape. The angular distribution of these domains is $W(\Delta)$ and, in many cases, is assumed to be gaussian (mosaic η).

(2) The extinction coefficient y_μ is defined by

$$P(n\,\mathrm{s}^{-1}) = J_0(n\,\mathrm{cm}^{-2}\,\mathrm{s}^{-1})\,\tilde{Q}(\mathrm{cm}^{-1})\,\Delta v(\mathrm{cm}^3)\,y_\mu,$$

where P denotes the diffracted power in the rocking curve method, J_0 is the incident intensity, and the macroscopic diffracting power is $\tilde{Q} \sim \lambda^3 N_c^2 F^2/\sin 2\theta$, where λ is the wavelength, F the structure factor, θ the Bragg angle and N_c the number of unit cells per cm^3. Further, Δv is the volume of the sample and y_μ the macroscopic extinction factor taking account of absorption (henceforth y_μ is assumed equal to y).

In fact, instead of considering the decrease of J_0 in the volume Δv of the crystal due to secondary extinction effects, we consider the integration of the diffracting cross section $\sigma(\epsilon)$ convoluted with the extinction function $\phi(\sigma)$ due to $\sigma(\epsilon)$:

$$y\tilde{Q} = \int \sigma(\epsilon)\,\phi(\sigma(\epsilon))\,\mathrm{d}\epsilon.$$

(3) BC derived $\sigma(\epsilon)$ for a convex crystal:

$$\sigma(\epsilon) = \frac{\tilde{Q}}{\Delta v}\int_{\Delta v} \frac{\sin^2 \pi\epsilon/\eta'}{(\pi\epsilon/\eta')^2}\,\frac{\mathrm{d}v}{\eta'}, \tag{1}$$

where η' is the broadening due to the finite dimension l of the diffracting region, so that $\eta' = \lambda/l \sin 2\theta = d/l \cos\theta$, where d is the (hkl) interspacing.

(4) The general solution allowing for multiple scattering (ETE) can be approximated by a power series in σ (see BC 18a, b), where terms with power $2p$ correspond to the $(2p)$-fold rescattering contribution.

(5) The cross section $\sigma(\epsilon)$ has to be averaged over the angular domain distribution $W(\Delta)$ of the mosaic model. The result is that the broadening of $\sigma(\epsilon)$ is generally the convolution of two parts, a particle size broadening η' and a mosaic broadening η. It is trivial to assume that

$$\eta''^2 = \eta'^2 + 2\pi\eta^2 .$$

(6) As y is the quantity of ultimate interest, an analytical expression is sought (BC 37):

$$y = \{1 + 2X + AX^2/(1 + BX)\}^{-\frac{1}{2}}, \tag{2}$$

where X describes the strength of the reflection (hkl); $X = \frac{2}{3}\tilde{Q}\bar{T}/\eta''$ (BC 42), with $\bar{T}$ the mean path length through the crystal.

Finally, to summarise this section, there exists a reasonable approximation of the ETE for crystals of general shape in the whole range of Bragg angles (BC 18a, b) and an analytical fit of y (BC 37) that can be used for either primary or secondary extinction.

3. Simple Calculations with a Simple Structure

At this stage of the discussion, it becomes useful to look at some practical calculations. To obtain a simple view of the intervening parameters, we examine the expression for the diffracted power with extinction correction expanded to the first order. For the primary extinction, one has with the preceding formalism (BC 37)

$$y_p = 1 - X_p, \qquad X_p = \tfrac{2}{3}\tilde{Q}l/\eta' = \tfrac{2}{3}(\lambda N_c F l)^2 . \tag{3}$$

For a given incident beam direction (a given ϵ), primary and secondary extinction effects may, to a first approximation, be considered independent. The same assumption used in averaging over various values of ϵ leads to $y \sim y_p(X_p)\, y_s(y_p X_s)$, which can be written as

$$y = \{1 - \tfrac{2}{3}(\lambda F N_c l)^2\}\left(1 - \tfrac{2}{3} y_p \frac{d}{\cos\theta} \frac{\lambda^2 (F N_c)^2 \bar{T}}{\{(d/l\cos\theta)^2 + 2\pi\eta^2\}^{\frac{1}{2}}}\right). \tag{4}$$

Then the diffracted power is written as

$$P = J_0 \tilde{Q} \Delta v\, y . \tag{5}$$

Let us now consider a single crystal of $AuCu_3$ ($\bar{T} \sim 0{\cdot}1$ cm) studied by neutron diffraction with $\lambda \sim 1$ Å. Table 1 gives the calculated diffraction schema for reflections at low and high angles ($a = 3{\cdot}74$ Å and $\eta = 1'$). The scattering lengths of Au and Cu are respectively $0{\cdot}763\times10^{-12}$ and $0{\cdot}769\times10^{-12}$ cm. The structure

Table 1. Calculated data for the $AuCu_3$ compound

	F	θ (deg.)	d (Å)	FN_c	$d/\cos\theta$ (Å)
100	I	7·7	3·74	$1·1\times10^{-4}$	3·77
111	II	13·4	2·16	0·059	2·22
620	II	57·7	0·59	0·059	1·10
621	I	58·9	0·58	$1·1\times10^{-4}$	1·12

factors fall into two groups: (I) superlattice reflections with mixed indices [Au–Cu: $F(\mathrm{I}) = -0·006\times10^{-12}$ cm]; and (II) fundamental reflections with (hkl) all even or all odd [Au+3Cu: $F(\mathrm{II}) = 3·07\times10^{-12}$ cm].

With the BC formalism, a strong secondary extinction appears for $\eta < 1'$ [$2\pi\eta^2 = (7·5\times10^{-4})^2$]; calculation shows that for $l \sim 0·20$ μm, the (111) reflection has an extinction mainly driven by the particle size η' and the (620) reflection has the same extinction mainly driven by the mosaic spread η. For $l \sim 1$ μm, the primary extinction of $F(\mathrm{II})$ is $y_p \sim 0·998$, but yields $y_p \sim 0·77$ for $l = 10$ μm; in all cases, the primary extinction of $F(\mathrm{I})$ is negligible. For $l \sim 1$ μm, the secondary extinction of the (111) reflection is $y_s \sim 0·34$, and $y_s \sim 0·66$ for the (620) reflection; in all cases, the secondary extinction of $F(\mathrm{I})$ is negligible.

This typical example shows the connection between the different parameters, and shows that the results are often surprising and change strongly with other experimental conditions (wavelength).

4. Experimental Tests of the BC Formalism

The failure to describe primary extinction in this kinematical model suggests that the BC formalism should be applied to severe extinction cases to test the reliability of the method. The problem is the adequacy of such tests. Essentially the secondary extinction correction must cancel the disproportion introduced by the extinction between strong and weak reflections. X rays, which concentrate strong reflections at low Bragg angles due to the form factor, the $\sin2\theta$ term, and thermal vibrations, cannot be a good tool to reveal extinction and to decide the best model; but with unpolarised neutrons, the absence of the form factor for the nuclear structure factor F_N, partially breaks the correlation between J_0, y and B.

The unique way to probe a model is to vary in a known way the parameters and to compare with the observed data. These parameters are the wavelength, the structure factors and the pathlength $\bar{T}$; the fitted parameters are the particle size, the mosaic spread and the shape of the distributions of $\sigma(\epsilon)$ and $W(\Delta)$. We now examine two experiments carried out by varying the wavelength or the structure factors.

(a) Change of the Wavelength

The experiment (Delapalme *et al.* 1978) was carried out during a study of the magnetisation density in URh_3 which has the $AuCu_3$ structure and, as discussed above, possesses two groups of structure factors. As a first attempt to assess the degree of extinction, integrated intensities were collected at $\lambda = 1·05$ Å on a conventional four-circle diffractometer at the Argonne National Laboratory. The resulting fit yielded $y_{min} \sim 0·3$. Because this value of y gives a large correction, we have further examined the extinction by measuring a limited set of integrated intensities at

$\lambda = 0{\cdot}757$ and $0{\cdot}527$ Å on the D9 four-circle diffractometer at ILL. The structure factors were then placed on an absolute scale by using the weak superlattice reflections, which exhibit negligible extinction. Finally, all structure factors were refined together with common extinction and thermal parameters.

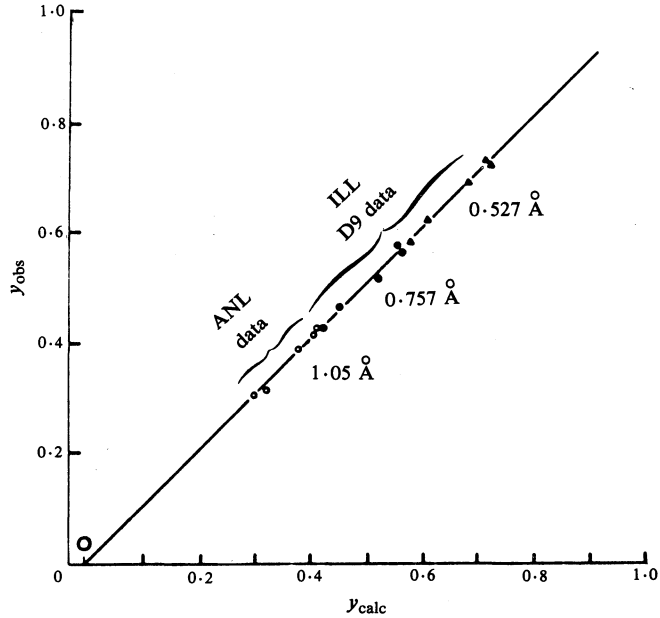

Fig. 1. Graph of y_{obs} versus y_{calc} from BC extinction theory for URh_3. Only the strong reflections at each wavelength are plotted: open circles, 1·05 Å; solid circles, 0·757 Å; and triangles, 0·527 Å. The weak reflections have $y > 0{\cdot}95$.

The first result was that the Zachariasen formula was inadequate to deal with the entire set of structure factors; for large extinction, y is overestimated. Using the BC formalism with the parameters $l = 14(3)$ μm and $\eta = 0{\cdot}34(3)'$ and with a Lorentzian shape for $\sigma(\epsilon)$, we obtained a residue (0·015) with thermal parameters $B_U = 0{\cdot}25(3)$ Å^2 and $B_{Rh} = 0{\cdot}32(3)$ Å^2. To illustrate the extent of agreement for the extinction, we have plotted y_{obs} against y_{calc} for the strong reflections from each wavelength experiment in Fig. 1. The result is surprisingly good considering the large range of variation in y_{obs} ($0{\cdot}3 \leqslant y \leqslant 0{\cdot}75$).

(b) Change of Structure Factor Values using Polarised Neutron Diffraction (BDBF)

In testing extinction effects, we saw that difficulties arise from the unknown values of the scale factor and thermal vibration parameters included in equation (5). Contrary to the X-ray case, neutron diffraction studies measure strong reflections over a large range of Bragg angle, thus avoiding biased correlations between y and the thermal parameters B. As pointed out by BDBF, polarised neutron experiments are an excellent tool for testing extinction models because one measures directly the absolute value of the cross-term between nuclear and magnetic structure factors. BDBF and Delapalme (1979) pointed out the experimental conditions where the flipping ratio R

can be simply written as the ratio of the diffracted power $P(\pm)$ for the up and down spins of incident neutrons:

$$R = \frac{P(+)}{P(-)} = \frac{F_+^2\, y^+}{F_-^2\, y^-} = \frac{(F_N+F_M)^2 y^+}{(F_N-F_M)^2 y^-} = R_o \frac{y^+}{y^-}. \tag{6}$$

where F_N and F_M are the nuclear and magnetic structure factors of a given reflection (hkl), and $y^\pm$ are the extinction corrections corresponding to $F_\pm$. In equation (6) it is assumed that an integration over ϵ has been performed by the wavelength band and the collimation.

For polarised neutrons, the flipping ratio measurements lead to an absolute value of R, without any scale factor, because we compare directly $P(+)$ and $P(-)$. Moreover, by utilising reflections at low Bragg angles where thermal parameters B are not of great importance and totally cancel for compounds with the same B values for the different atoms, we note that for ferro- or ferri-magnetic centrosymmetric structure with $|R-1| > 0{\cdot}1$, polarised neutron experiments are very dependent on extinction and provide original tests for extinction models.

Writing equation (6) as

$$R = R_o\, y^+/y^- = R_o\{1-e(l,\eta)\}, \tag{7}$$

we show that one can calculate R from a linear relationship of its kinematical value R_o, where e is a function of the particle size, the mosaic spread and the shape of the distributions for $\sigma(\epsilon)$ and $W(\Delta)$.

In other words, if one knows the right expression to correct for the extinction, it is possible to find only two adjustable parameters (l and η) which align perfectly all experimental values of R along the line of (7); the reliability of the model used to correct the extinction can be judged from the deviation of the experimental R values from the calculated relation (7).

In the practical case of our study on yttrium–iron–garnet (YIG) (BDBF), the fact that we could consistently align the experimental R values corresponding to different crystals (1, 2, 3, 4), different thicknesses and different wavelengths, with only two fitted parameters [$l \sim 17(3)\ \mu$m and $\eta \sim 6(3)''$] and a Lorentzian distribution for $\sigma(\epsilon)$, suggests that this type of correction could be quite general (see Fig. 2). Detailed experimental information can be found in BDBF and Delapalme (1979).

5. Detection and Correction

An important step in visualising extinction effects is to consider Fig. 3 which shows that there is a progressive deviation of the observed reflecting power $\mathscr{R}_o$ from the calculated $\mathscr{R}_c = \tilde{Q}\bar{T}/\eta''$. For example, looking at $\mathscr{R}_{c1}$, we observe $\mathscr{R}_{o1}$ which leads to the conclusion of no extinction effects. But looking at $\mathscr{R}_{c2}$, we observe $\mathscr{R}'_{o2}$ instead of the real value $\mathscr{R}_{o2}$. For polarised neutron experiments, one sees that measuring a theoretical value $R_c \sim \mathscr{R}^+_{c2}/\mathscr{R}^-_{c2}$, we observed $R'_o \sim \mathscr{R}'^+_{o2}/\mathscr{R}'^-_{o2}$ instead of $R_o \sim \mathscr{R}^+_{o2}/\mathscr{R}^-_{o2}$. In other words, assuming that we can write (4) as $y^\pm = 1-KF^2_\pm$, for small values of $\gamma = F_M/F_N$ the flipping ratio can be written as

$$R \sim (1+4\gamma)\{1-K(F_+^2-F_-^2)\} = (1+4\gamma)\{1-4KF_N^2\gamma\},$$

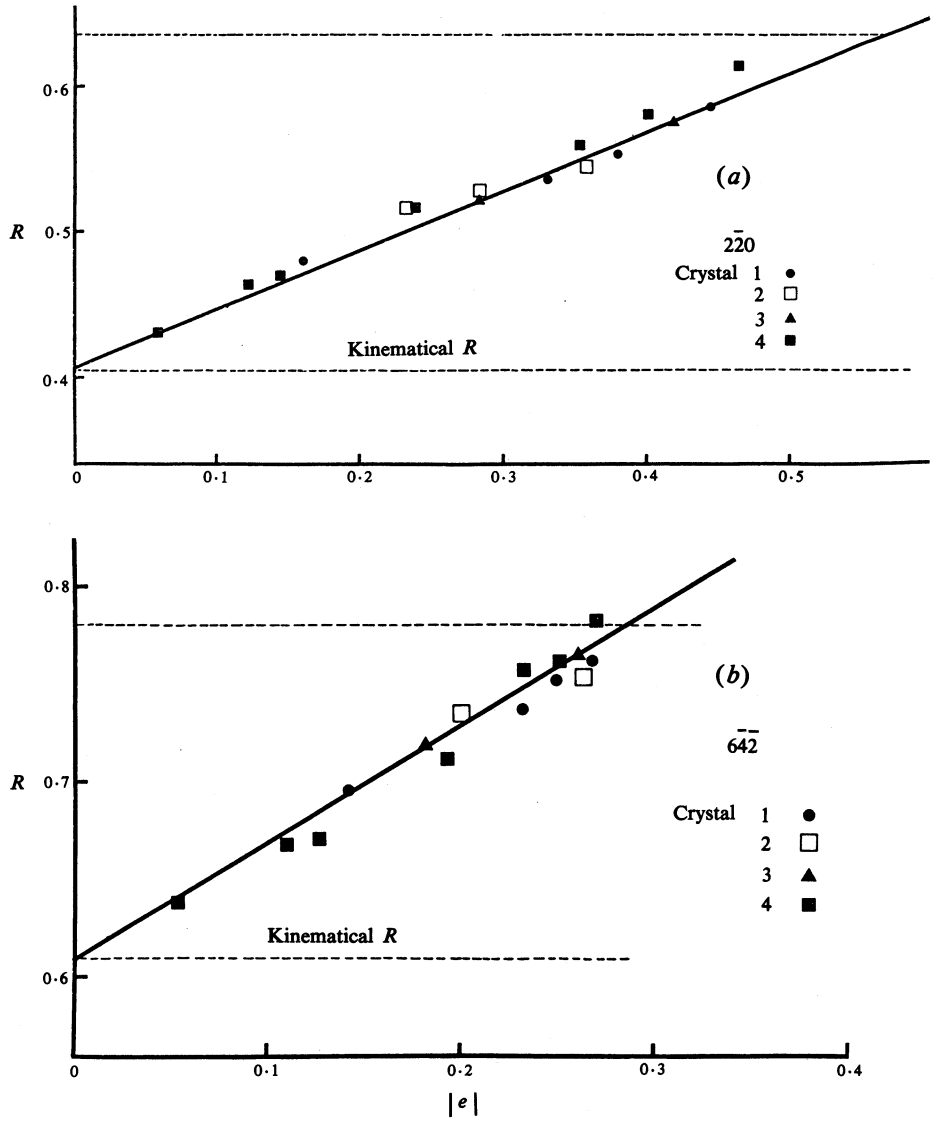

Fig. 2. Measured flipping ratio R as a function of $|e|$ with a Lorentzian extinction correction for four samples of yttrium–iron–garnet: YIG-1 (circles), YIG-2 (open squares), YIG-3 (triangles) and YIG-4 (solid squares). A comparison with the straight line (7) is made for (*a*) $2\bar{2}0$ and (*b*) $6\bar{4}\bar{2}$ reflections.

and can be seriously damped by the term in braces, which represents the calculated extinction correction for very small γ values.

Moreover, we can conceive of cases where $4KF_N^2\gamma$ becomes negligible but is equal to 4γ; in these cases negligible extinction leads to a 100% extinction correction. This effect has been seen often with magnetisation density measurements of compounds in a weak paramagnetic state.

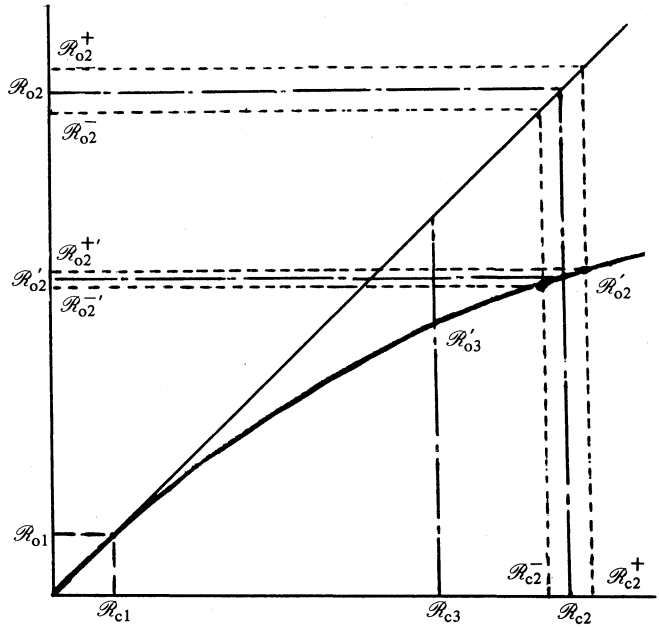

Fig. 3. Observed reflecting power $\mathscr{R}_o$ versus calculated $\mathscr{R}_c$. Extinction effects correspond to the deviation from the first bisector.

6. Limiting Cases and Conclusions

We saw that Fig. 3 is an important tool in understanding extinction effects. For two samples, a metallic compound URh_3 and the YIG oxide, we showed that a good extinction correction can be applied with reasonable fitted parameters ($1 \leqslant l \leqslant 15\ \mu m$ and $0{\cdot}1 < \eta < 1'$). Finally, in the case of polarised neutron experiments, we saw that an important change in the value of the structure factors ($\pm F_M$) is a reliable test to evaluate the best extinction correction for a given sample [Lorentzian shape for $\sigma(\epsilon)$ in the case of YIG]. It remains that the detection of extinction effects depends on the variation of $\mathscr{R}'_{o2}$ or R'_{o2} with the wavelength. Indeed, the wavelength is the only other parameter which can be varied easily without sample modification.

However, one sees clearly in Fig. 3 that, if the extinction is very strong (strong F_N), only good statistics in the measurement of $\mathscr{R}'_o$ or R'_o can detect significant changes with the wavelength and, in some cases (small F_M), the change of $\mathscr{R}'_{o3} - \mathscr{R}'_{o2}$ can be more easily obtained than that of $R'_{o3} - R'_{o2}$.

Finally, if it is meaningful to correct for extinction within the BC formalism, it is useful to draw the universal curve of Fig. 3 and then to have an estimate of the degree of extinction in a particular experiment; moreover, this curve can disclose which is the most reliable experiment to obtain the fitted parameters (l, η) and to correct for extinction effects.

As pointed out by Kato (1976, 1979, 1980) and Kulda (1984, 1987), there remains the important failure to describe primary extinction. Models based on elastically deformed domains are certainly welcome, but the difficulty will remain for a long time of finding the experimental conditions of real primary extinction to test these new models.

References

Becker, P. J. (1977). *Acta Cryst.* A **33**, 667–71.
Becker, P. J., and Coppens, P. (1974). *Acta Cryst.* A **30**, 129–47.
Bogdanov, S. G., and Menshikov, A. Z. (1976). *Acta Cryst.* A **32**, 869–76.
Bonnet, M., Delapalme, A., Becker, P., and Fuess, H. (1976). *Acta Cryst.* A **32**, 945–53.
Delapalme, A. (1979). *Nukleonika* **24**, 723–36.
Delapalme, A., Lander, G. H., and Brown, P. J. (1978). *J. Phys.* C **11**, 1441–50.
Dietrich, O. W., and Als-Nielsen, J. (1965). *Acta Cryst.* **18**, 184–9.
Kato, N. (1976). *Acta Cryst.* A **32**, 453–66.
Kato, N. (1979). *Acta Cryst.* A **35**, 9–16.
Kato, N. (1980). *Acta Cryst.* A **36**, 171–7.
Kulda, J. (1984). *Acta Cryst.* A **40**, 120–6.
Kulda, J. (1987). *Acta Cryst.* A **43**, 167–73.
Schneider, J. R. (1974). *J. Appl. Cryst.* **7**, 541; 547–54.
Takagi, S. (1969). *J. Phys. Soc. Jpn* **26**, 1239–53.
Werner, S. A. (1974). *J. Appl. Phys.* **45**, 3246–54.
Zachariasen, W. H. (1967). *Acta Cryst.* **23**, 558–65.
Zachariasen, W. H. (1968). *Acta Cryst.* A **24**, 421–4.

Manuscript received 25 August, accepted 13 November 1987